



Published in final edited form as:

ACS Nano. 2015 December 22; 9(12): 11812–11819. doi:10.1021/acsnano.5b03923.

Characterization of Interstrand DNA-DNA Cross-Links Using the α -Hemolysin Protein Nanopore

Xinyue Zhang[†], Nathan E. Price[‡], Xi Fang[†], Zhiyu Yang[‡], Li-Qun Gu^{†,*}, and Kent S. Gates^{‡,§,*}

[‡]University of Missouri, Department of Chemistry, 125 Chemistry Building, Columbia, MO 65211

[§]University of Missouri, Department of Biochemistry, Columbia, MO 65211

[†]University of Missouri, Department of Bioengineering and Dalton Cardiovascular Research Center, Columbia, MO 65211

Abstract

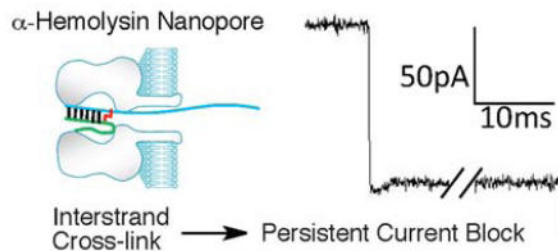
Nanopore-based sensors have been studied extensively as potential tools for DNA sequencing, characterization of epigenetic modifications such as 5-methylcytosine, and detection of microRNA biomarkers. In the studies described here, the α -hemolysin protein nanopore embedded in a lipid bilayer was used for the detection and characterization of interstrand cross-links in duplex DNA. Interstrand cross-links are important lesions in medicinal chemistry and toxicology because they prevent the strand separation that is required for read-out of genetic information from DNA in cells. In addition, interstrand cross-links are used for the stabilization of duplex DNA in structural biology and materials science. Cross-linked DNA fragments produced unmistakable current signatures in the nanopore experiment. Some cross-linked substrates gave irreversible current blocks of >10 min, while others produced long current blocks (10–100 s) before the double-stranded DNA cross-link translocated through the α -hemolysin channel in a voltage-driven manner. The duration of the current block for the different cross-linked substrates examined here may be dictated by the stability of the duplex region left in the vestibule of the nanopore following partial unzipping of the cross-linked DNA. Construction of calibration curves measuring the frequency of cross-link blocking events ($1/\tau_{on}$) as a function of cross-link concentration enabled quantitative determination of the amounts of cross-linked DNA present in samples. The unique current signatures generated by cross-linked DNA in the α -HL nanopore may enable the detection and characterization of DNA cross-links that are important in toxicology, medicine, and materials science.

Graphical abstract

*Address correspondence to: gatesk@missouri.edu; phone: (573) 882-6763 and gul@missouri.edu; phone: (573) 882-2057.

Conflict of Interest: The authors declare no competing financial interest.

Supporting Information Available: Results of experiments showing the current blocks for single-stranded DNA, un-cross-linked duplex DNA, and persistent blocks by duplexes D6 and D8. Examination of D8 at higher applied potentials, analysis of dwell times for D3, and gel electrophoretic analysis of cross-link yield in duplex D7. This material can be found free of charge *via* the Internet at <http://pubs.acs.org>



Keywords

Damaged DNA; interstrand cross-link; nanopore; α -hemolysin; abasic site

Nanopore-based sensors have been studied extensively as potential tools for DNA sequencing, characterization of epigenetic modifications such as 5-methylcytosine, and detection of microRNA biomarkers.^{1–10} To date, relatively few studies have employed nanopores for the detection and characterization of covalently modified DNA. Most notably, Burrows and White have used the α -hemolysin (α -HL) nanopore embedded in a lipid bilayer to characterize important features of abasic, 8-oxo-7,8-dihydroguanine, spiroiminodihydantoin, guandinohydantoin, and *N*²-benzo[a]pyrene-modified guanine residues in DNA.^{11–18} Nanopore technology may provide a useful approach for analysis of diverse covalent DNA modifications that are important in toxicology and medicine.^{19–24}

Here we describe the use of a protein nanopore to characterize interstrand cross-links in duplex DNA. Interstrand cross-links are important in biology because they block strand separation that is required for read-out of genetic information from DNA in cells.^{25–28} In addition, interstrand cross-links have been used for the stabilization of duplex DNA in structural biology and materials science applications.^{29–36} There exist a wide structural variety of DNA-DNA cross-links that are important in toxicology, medicine, structural biology, and materials science.^{25,26,32,35–37} The detection and characterization of interstrand cross-links in DNA is a challenging task. Typically, full characterization of an interstrand DNA cross-link requires a diverse array of techniques that may include gel electrophoresis, LC-MS, spectroscopic monitoring of thermal denaturation, chemical synthesis, multi-dimensional NMR, and X-ray crystallography. Recognizing the power of nanopores to detect subtle differences in nucleic acid structure, we felt that this technology might provide a useful tool for analyzing the occurrence and properties of interstrand cross-links in double-stranded DNA.

In our studies, we used the α -HL ion channel nanopore embedded in a lipid bilayer to characterize DNA cross-links.^{38–40} The α -HL pore is 10 nm long and consists of a 2.4 nm wide entrance that gives way to a “vestibule” that reaches 4.6 nm in width before narrowing to a constriction of 1.4 nm (Figure 1).³⁹ Under electrophoretic force, single-stranded DNA fragments pass rapidly (1–20 μ s/nucleotide (nt)) through the pore’s narrow constriction. On the other hand, approximately 10 base pair (bp) of duplex DNA can enter the vestibule but, at 2 nm in width, the double helix is too big to pass through the pore and must undergo a relatively slow (100–2000 μ s/nt) “unzipping” process before the two strands can separately

translocate through the pore.^{1–4,6,38,40–42} Passage of DNA through the α -HL pore causes a transient decrease in the ion current. The extent and duration of the current decrease combine to make up the “current signature” of the DNA translocation event for a particular substrate.^{1–4,6,38,40–42} Prior to this work, the nature of the current signature(s) that might be produced by DNA duplexes containing interstrand cross-links was unknown. The results described here demonstrate that interstrand DNA-DNA cross-links can be clearly and quantitatively detected using the α -HL protein nanopore. The unique current signatures generated by cross-linked DNA in the α -HL nanopore may enable the detection and characterization of DNA cross-links that are important in toxicology, medicine, and materials science.

RESULTS AND DISCUSSION

Preparation of Cross-linked DNA Substrates. The interstrand cross-links examined here were generated by the reaction of a guanine residue with the aldehyde group of an abasic site on the opposing strand of duplex DNA in the presence of NaCNBH_3 (Scheme 1).^{43,44} The chemical structure and stability of the reduced dG-Ap cross-link recently has been established.⁴⁵ A series of oligomeric duplexes were generated in which the location of the cross-link 1 was varied with respect to a poly-dC₃₀ tail (Table 1). Threading of the poly-dC₃₀ overhang into the pore facilitates capture of the duplexes by the α -HL nanopore and guides the duplex region of the substrate into the vestibule.⁶

Duplexes D7 and D8 Cause Persistent Current Blocks. We first showed that the single-stranded oligonucleotides used in these studies generated short current blocks (Figures S1 and S2). For example, the longer strand of duplex D7 generated current blocks of 160 ± 100 μs as it passed through the α -HL channel (Figures 2, S1, and S2). We also examined the current blocks induced by un-cross-linked duplexes (Figures S3 and S4). The un-cross-linked duplex D7 generated multi-level current blocks corresponding to trapping of the duplex, unzipping, and passage of the longer (poly-dC-containing) strand, followed by translocation of the shorter, displaced strand (Figures 2, S3, and S4). The duration of the current blocks induced by the duplex was 6.6 ± 1.2 ms (up to 100-fold longer than the block generated by passage of single-stranded DNA through the pore).

We then analyzed a reaction mixture containing the cross-linked duplex D7. The cross-linkage in this substrate was located near the center of the double-stranded domain. Three different types of current-blocking events were observed in the reaction mixture (Figure 2). First, we detected very short events giving a residual current of $12.6 \pm 1.1\%$, corresponding to the translocation of unhybridized single-stranded DNA in the mixture (Figure 2). Second, we observed the expected longer blocking events corresponding to the capture, unzipping, and translocation of the un-cross-linked duplex (with a residual current of $11.2 \pm 1.3\%$, Figure 2). The third type of event was a persistent block (>10 min) that we ascribed to the cross-linked duplex (Figure 2). Careful inspection of the current signature for the persistent block revealed that this event was composed of two different states. The initial and deepest current block presumably corresponds to passage of the poly-dC₃₀ tail through the pore (with a residual current of $11.1 \pm 0.6\%$, Figure 2b). The second state involved a slight recovery of current likely corresponding to the partially unzipped duplex with the cross-link

structure 1 “wedged” at the narrow constriction of the α -HL pore (with a residual current of $15.5 \pm 1.1\%$, Figure 2b). At this point, reversal of the voltage polarity allowed the cross-link to be “backed out” of the channel, leaving the pore open and ready to trap another duplex when the polarity was reset (Figure 2b). To confirm that the persistent blocks could be assigned to the cross-linked duplex in the mixture, we showed that the purified, cross-linked duplex D7 did, indeed, generate persistent current blocks (Figure S5). Figure 3 shows a multi-channel experiment in which multiple α -HL pores embedded in a lipid bilayer were sequentially and irreversibly blocked by the D7 duplex. The behavior of duplex D8, in which the cross-link was located only 3 nt away from the poly-dC tail, was similar to duplex D7, causing a persistent current block after capture in the pore (Table 1, Figure S6). In fact, there was no evidence for translocation of D8 even when the applied voltage was increased from 120 to 180 mV over the course of 30 min (Figure S7).

Duplex D3 Causes Long-Lasting, Yet Transient, Current Blocks. Interestingly, the cross-linked duplex D3 displayed properties very different from D7 and D8. The cross-link in D3 is distal to the poly-dC tail, located only four bp from the end of the duplex (Table 1). Trapping of D3 in the pore induced a deep and long-lasting current block – however, the duration of the block caused by D3 was quite different from that caused by duplexes D7 and D8 (Figures 4 and S5). Specifically, where the current blocks caused by trapping of D7 and D8 in the nanopore can persist for >30 min, the block induced by D3 typically lasted between 10–100 sec (Figure S8). The current signature for the blocking event caused by D3 consists of three distinct states (Figure 4c). The first two states (with residual currents of $9.5 \pm 1.0\%$ and $14.1 \pm 1.0\%$) closely resemble those observed for duplex D7, described above. These involve an initial current block corresponding to passage of the poly-dC tail through the pore (Figure 4d), followed by a slight recovery in the current flow corresponding to the partially unzipped duplex with the cross-link wedged at the narrow constriction of the α -HL pore (Figure 4d). Most striking, this state was followed by a nearly complete block in current flow (with a residual current of $2.6 \pm 0.8\%$) and then re-opening of the channel. We suggest that melting of the four bp duplex in the vestibule of the pore enables a conformational adjustment that allows the cross-link to squeeze through the pore (Figure 4d). The tight fit of the reduced dG-Ap lesion 1 as it passes through the narrow constriction of α -HL pore presumably is responsible for the unique current signature involving nearly complete blockage. We found that, when a higher voltage was applied, the dwell time of the cross-linked duplex D3 in the pore was decreased, consistent with the interpretation that the cross-link translocates from the *cis* to the *trans* side of the pore (Figure 4b). Breakage of covalent carbon-carbon ($H^\circ > 80$ kcal/mol) or carbon-nitrogen bonds ($H^\circ > 70$ kcal/mol) in the cross-link is quite unlikely under the conditions used here.

Evidence That Duration of the Current Block Is Determined By the Stability of the Duplex Trapped in the Nanopore Following Partial Unzipping of the Cross-linked Substrate. We suggest that, when partial unzipping of the cross-linked substrate leaves a stable region of duplex DNA in the vestibule of the pore, the conformational reorganization required to enable passage through the pore is inhibited and a persistent current block results (e.g. D6–D8, Table 1). On the other hand, melting of an unstable duplex region in the vestibule following partial unzipping enables the conformational reorganization required for passage of the cross-link through the pore as seen in the case of D3. Consistent with this hypothesis,

the duration of the block induced by duplexes D1–5 correlated with the calculated thermal stability of the duplex remaining in the vestibule of the pore when the cross-linked substrate is stalled at the constriction after partial unzipping (Table 1, Figure 5). The length of the “arms” trapped in the vestibule also appears to affect the dwell time of the cross-linked duplexes. For example, the residual duplex in D4 has a lower melting temperature than D5, yet D4 displays a longer current block than D5. The longer arms of D4 (6–7 nt in D4 versus 4–5 nt in D5) may sterically hinder the structural reorganization required for the cross-link to pass through the pore constriction. Of course, the kinetic stability of the residual duplex trapped in the vestibule may be a key factor in determining the dwell time of different cross-linked duplexes. Duplex D6, containing a structurally distinct cross-link between 2'-deoxyadenosine and the abasic site,^{46,47} also presented a persistent current block to the α -HL pore (Table 1 and Figure S6).

Quantitative Detection of Cross-linked Duplex D7 in a Mixture. Finally, we used the α -HL nanopore to estimate the cross-link yield in a sample containing both native and cross-linked duplex D7 (Figure 6). As noted above, analysis of cross-linking reaction mixtures revealed three different types of blocking events (Figure 2). The nanopore can be used as a molecular counter, with the frequency of each type of blocking event corresponding to the relative concentration of each species. The exponential fit of the distribution of time intervals between each type of blocking event allowed calculation of the corresponding association rates. In multichannel experiments, the time course for sequential and irreversible blocking of pores could be fit to the equation: $y = y_0 + Ae^{-t/\tau_{on}}$ (Figure 6a). Blocking by D7 is irreversible (Figure S5) and the use of purified standards for cross-linked and native duplex allowed us to determine the relationship between frequency and concentration for D7 (Figure 6b). With this information in hand, we used the nanopore to measure the yield of cross-linked DNA generated in an actual cross-linking reaction. The cross-link yield calculated from the nanopore data ($9.0 \pm 1.7\%$) matched well with those obtained by parallel gel electrophoretic analysis the reaction mixtures ($10.8 \pm 0.8\%$, Figure S9).

Comparison of Cross-linked Duplexes with Blunt Ends or a Four-base Overhang. It is interesting to compare the properties of cross-linked duplexes lacking the long dC₃₀ tails present in duplexes D1–8. We found that a duplex analogous to D7, but lacking the dC₃₀ tail caused long blocks (3.2 ± 0.4 s) at an applied voltage of 120 mV (Figure S10). Interestingly, the blocks were reversible and there was substantial current fluctuation during the block. The block consists of two states. The first state with a residual current of $26.7 \pm 1.2\%$ may arise from the duplex lodged in the vestibule of the pore. A similar model has been invoked to explain the long-lasting current blocks (~25% residual current) induced by blunt-ended 22 and 60 bp duplexes in the α -HL channel.^{41,48} The second state observed for the blunt-ended version of D7 in our experiments, with a residual current of $12.4 \pm 1.4\%$, likely corresponded to the partially unzipped duplex threaded into the pore constriction.⁴¹ Evidently, without the dC₃₀ tail, the partially unzipped blunt-ended duplex is held less strongly in the pore, making the blocking event reversible. Consistent with this view, when the potential was increased from 120 to 150 mV, the block duration became very long (> 1 min) and was relieved only when the polarity of the applied voltage was reversed and the cross-linked DNA “backed out” of the pore (Figure S11). The current signature of the cross-linked, blunt-end duplex was clearly distinct from the current signature induced by an

analogous un-cross-linked, blunt-end duplex (Figure S13) which is fully unzipped followed by translocation through the pore. Evidence for unzipping of the un-cross-linked, blunt-end duplex was provided by the decrease in block duration as the voltage increases⁴¹ and observation of a characteristic current signature that has been dissected previously.^{6,41,42} These results yield two important insights: i. in duplexes containing dC₃₀ tails, capture of the duplexes occurs *via* threading of the tail into the pore and there are relatively few signals (< 10%) that correspond to blunt-end-first capture and, ii. the blunt-ended 21 bp duplex containing an interstrand cross-link can be recognized by its distinct current-blocking signature. Similar results were obtained for a cross-linked duplex bearing a four-nucleotide overhang (Figure S12).

CONCLUSIONS

In conclusion, our work provides characterization of DNA-DNA interstrand cross-links using nanopore technology. Importantly, the results show that interstrand DNA cross-links can be clearly and quantitatively detected using the α -HL nanopore. Interestingly, the exact nature of the current signature depends on the location of cross-link within the duplex fragment. When partial unzipping leaves a stable region of duplex DNA trapped in the vestibule of the α -HL pore, a persistent current block was observed. On the other hand, when partial unzipping of the cross-linked DNA substrate leaves a short duplex region in the vestibule, melting of these base pairs enables a conformational adjustment that allows the reduced dG-Ap lesion to squeeze through the pore, causing a period of complete current blockage prior to reopening of the channel.

It remains to be seen whether structurally distinct cross-links will display different current signatures in the α -HL nanopore, but we anticipate that this will be the case. In this regard, nanopore measurements have the potential to help shed light on cross-link structure and properties. In future studies, it may be of interest to examine cross-links derived from clinically-used anticancer drugs such as cisplatin, cyclophosphamide, and bendamustine. In addition, it would be interesting to explore the utility of small, solid-state nanopores for these applications. Nanopore technology may offer a tool for the rapid screening of cross-linking agents in drug discovery and development. Importantly, the yields of cross-links generated in cellular DNA may correlate with therapeutic efficacy for some drugs^{49–53} and nanopore-based sensing may ultimately offer a practical alternative to approaches such as the comet assay⁵⁴ for the quantitative detection of DNA cross-links in clinical samples.

METHODS

Materials

All chemicals including KCl, Tris-HCl, MgCl₂, pentane, sephadex, and hexadecane were obtained from Sigma-Aldrich (St. Louis, MO, USA) and were used as received. The compound 1,2-diphytanoyl-sn-glycero-3-phosphocholine used for lipid bilayer formation was from Avanti Polar Lipids (Alabaster, AL, USA) and was used without further purification. Oligonucleotides were purchased from Integrated DNA Technologies (Coralville, IA). All enzymes were purchased from New England Biolabs (Ipswich, MA, USA). [γ -³²P]-ATP (6000 Ci/mmol) was purchased from Perkin Elmer. Quantification of

radioactivity in polyacrylamide gels was carried out using a Personal Molecular Imager (BIORAD) with Quantity One software (v.4.6.5).

Electrophysiology Measurements

A membrane of 1,2-diphytanoyl-*sn*-glycero-3-phosphocholine was formed on a small orifice of approximately 150 μm diameter in a Teflon partition that separates two identical Teflon chambers. Each chamber contained 2 mL of electrolyte solution (1 M KCl, 10 mM Tris-HCl, pH 7.4). Less than 1 μL of α -hemolysin was added to the *cis* chamber with stirring, after which, a conductance increase indicated the formation of a single channel. For multichannel recording, 2 to 5 μL of α -hemolysin was added. The ionic current through the α -hemolysin protein nanopore was recorded by an Axopatch 200B amplifier (Molecular Devices Inc., Sunnyvale, CA), filtered with a built-in 4-pole low-pass Bessel Filter at 5 kHz, and finally acquired into the computer using a DigiData 1440A A/D converter (Molecular Devices) at a sampling rate of 20 kHz. All the data recording and acquisition including single channel, multichannel and persistent blocking recording of DNA cross-links were controlled through a Clampex program (Molecular Devices) and the analysis of nanopore current traces was performed using Clampfit software 10.4 (Molecular Devices).

Preparation of Cross-linked DNA Substrates

The complementary oligonucleotides for each duplex were annealed⁵⁵ at a 1:1 molar ratio and treated with the enzyme UDG (50 units/mL, final concentration) to generate Ap sites.^{56,57} The enzyme UDG was removed by phenol-chloroform extraction and the DNA ethanol precipitated and the pellet washed with 80% EtOH-water.⁵⁵ The resulting Ap-containing DNA duplexes were redissolved in a buffer composed of HEPES (50 mM, pH 7) containing NaCl (100 mM) and incubated at 37 °C for 120 h. Reaction mixtures were then analyzed in the nanopore experiments. In some cases, parallel denaturing polyacrylamide gel electrophoretic analysis of the cross-linking reaction mixture was carried out as previously described.^{46,47} Briefly, the DNA was ethanol precipitated⁵⁵ and 5'-³²P-labeled using standard procedures.⁵⁵ After ³²P-labeling, the protein was removed by phenol-chloroform extraction and the sample desalted by passage through sephadex G-25. The samples were then mixed with formamide loading buffer,⁵⁵ loaded into the wells of a 20% denaturing polyacrylamide gel, and gel electrophoresed for 6 h at 1000 V. The amount of radiolabeled DNA in each band from the gel was measured by phosphorimager analysis. Isolation of the cross-linked DNA from polyacrylamide gels, for use in constructing calibration curves, was carried out as described previously.⁴⁶

Supplementary Material

Refer to Web version on PubMed Central for supplementary material.

Acknowledgments

We are grateful to the National Institutes of Health for support of this work (grants ES021007 to KSG and GM 079613 and GM 114204 to LQG). We thank Dr. John S. Oliver (Nabsys Inc.) for critical review of the manuscript.

REFERENCES AND NOTES

1. Branton D, Deamer DW, Marziali A, Bayley H, Benner SA, Butler T, Di Ventra M, Garaj S, Hibbs A, Huang X, et al. The Potential and Challenges of Nanopore Sequencing. *Nat Biotech.* 2008; 26:1146–1153.
2. Laszlo AH, Derrington IM, Brinkerhoff H, Langford KW, Nova IC, Samson JM, Barlett JJ, Pavlenok M, Gundlach JH. Detection and Mapping of 5-Methylcytosine and 5-Hydroxymethylcytosine With Nanopore MspA. *Proc Nat Acad Sci USA.* 2013; 110:18904–18909. [PubMed: 24167255]
3. Venkatesan BM, Bashir R. Nanopore Sensors for Nucleic Acid Analysis. *Nat Biotech.* 2012; 6:615–624.
4. Clarke J, Wu HC, Jayasinghe L, Patel A, Reid S, Bayley H. Continuous Base Identification for Single-Molecule Nanopore DNA Sequencing. *Nat Nanotech.* 2009; 4:265–270.
5. Kang I, Gu LQ. Single Protein Molecule Detection with a Transfer-APTamer (Piston) Sliding in a Protein Pore. *Biophys J.* 2012; 102:727a.
6. Wang Y, Zheng D, Tan Q, Wang MX, Gu LQ. Nanopore-Based Detection of Circulating microRNAs in Lung Cancer Patients. *Nat Nanotech.* 2011; 6:668–674.
7. Laszlo AH, Derrington IM, Ross BC, Brinkerhoff H, Adey J, Nova IC, Craig JM, Langford KW, Samson JM, Daza R, et al. Decoding Long Nanopore Sequencing Reads of Natural DNA. *Nat Biotech.* 2014; 32:829–833.
8. Manrao EA, Derrington IM, Laszlo AH, Langford KW, Hopper MK, Gillgren N, Pavlenok M, Niederweis M, Gundlach JH. Reading DNA at Single-Nucleotide Resolution with a Mutant MspA Nanopore and phi29 DNA Polymerase. *Nat Biotech.* 2012; 30:349–353.
9. Cherf GM, Lieberman KR, Rashid H, Lam CE, Karplus K, Akeson M. Automated Forward and Reverse Ratcheting of DNA in a Nanopore at 5-Å Precision. *Nat Biotech.* 2012; 30:344–348.
10. Wang Y, Luan B-Q, Yang Z, Zhang X, Ritzo B, Gates KS, Gu L-Q. Single Molecule Investigation of Ag⁺ Interactions with Single Cytosine-, Methylcytosine- and Hydroxymethylcytosine-Cytosine Mismatches in a Nanopore. *Sci Rep.* 2014; 4:1038/srep05883
11. Perera RT, Fleming AM, Johnson RP, Burrows CJ, White HS. Detection of Benzo[a]pyrene-guanine Adducts in Single-stranded DNA Using the α -Hemolysin Nanopore. *Nanotechnology.* 2015; 26:74002.
12. Johnson RP, Fleming AM, Burrows CJ, White HS. Effect of an Electrolyte Cation on Detecting DNA Damage with the Latch Constriction of α -Hemolysin. *J Phys Chem Lett.* 2014; 5:3781–3786. [PubMed: 25400876]
13. Jin Q, Fleming AM, Ding Y, Burrows CJ, White HS. Structural Destabilization of DNA Duplexes Containing Single-Base Lesions Investigated by Nanopore Measurements. *Biochemistry.* 2013; 52:7870–7877. [PubMed: 24128275]
14. Wolna AH, Fleming AM, An N, He L, White HS, Burrows CJ. Electrical Current Signatures of DNA Base Modifications in Single Molecules Immobilized in the α -Hemolysin Ion Channel. *Isr J Chem.* 2013; 53:417–430. [PubMed: 24052667]
15. An N, White HS, Burrows CJ. Modulation of the Current Signatures of DNA Abasic Site Adducts in the α -Hemolysin Ion Channel. *Chem Comm.* 2012; 48:11410–11412. [PubMed: 23076012]
16. An N, Fleming AM, White HS, Burrows CJ. Crown Ether-electrolyte Interactions Permit Nanopore Detection of Individual DNA Abasic Sites in Single Molecules. *Proc Nat Acad Sci USA.* 2012; 109:11504–11509. [PubMed: 22711805]
17. Jin Q, Fleming AM, Burrows CJ, White HS. Unzipping Kinetics of Duplex DNA Containing Oxidized Lesions in an α -Hemolysin Nanopore. *J Am Chem Soc.* 2012; 134:11006–11011. [PubMed: 22690806]
18. An N, Fleming AM, White HS, Burrows CJ. Nanopore Detection of 8-Oxoguanine in the Human Telomere Repeat Sequence. *ACS Nano.* 2015; 4:4296–4307. [PubMed: 25768204]
19. Gates KS. An Overview of Chemical Processes That Damage Cellular DNA: Spontaneous Hydrolysis, Alkylation, and Reactions with Radicals. *Chem Res Toxicol.* 2009; 22:1747–1760. [PubMed: 19757819]

20. Palchadhuri R, Hergenrother PJ. DNA As a Target for Anticancer Compounds: Methods to Determine the Mode of Binding and the Mechanism of Action. *Curr Opin Biotechnol.* 2007; 18:497–503. [PubMed: 17988854]
21. Enoch SJ, Cronin MTD. A Review of the Electrophilic Reaction Chemistry Involved in Covalent DNA Binding. *Crit Rev Toxicol.* 2010; 40:728–748.
22. Cheung-Ong K, Giaever G, Nislow C. DNA-Damaging Agents in Cancer Chemotherapy: Serendipity and Chemical Biology. *Chem Biol.* 2013; 20:648–659. [PubMed: 23706631]
23. Hurley LH. DNA and Its Associated Processes as Targets for Cancer Therapy. *Nature Rev Cancer.* 2002; 2:188–200. [PubMed: 11990855]
24. Dipple A. DNA Adducts of Chemical Carcinogens. *Carcinogenesis.* 1995; 16:437–441. [PubMed: 7697795]
25. Schärer OD. DNA Interstrand Crosslinks: Natural and Drug-induced DNA Adducts that Induce Unique Cellular Responses. *ChemBioChem.* 2005; 6:27–32. [PubMed: 15637664]
26. Rajski SR, Williams RM. DNA Cross-linking Agents as Antitumor Drugs. *Chem Rev.* 1998; 98:2723–2795. [PubMed: 11848977]
27. Muniandy PA, Liu J, Majumdar A, Liu S-t, Seidman MM. DNA Interstrand Crosslink Repair in Mammalian Cells: Step by Step. *Crit Rev Biochem Mol Biol.* 2010; 45:23–49. [PubMed: 20039786]
28. Clauson C, Schärer OD, Niedernhofer LJ. Advances in Understanding the Complex Mechanisms of DNA Interstrand Cross-link Repair. *Cold Spring Harbor Perspectives in Biology.* 2013; 5:a012732/1–a012732/25. [PubMed: 24086043]
29. Tomás-Gamasa M, Serdjukow S, Su M, Müller M, Carell T. "Post-It" Type Connected DNA Created with a Reversible Covalent Cross-link. *Angew Chem Int Ed Eng.* 2014; 53:796–800.
30. Ferentz AE, Keating TA, Verdine GL. Synthesis and Characterization of Disulfide Cross-linked Oligonucleotides. *J Am Chem Soc.* 1993; 115:9006–9014.
31. McManus FP, Khaira A, Noronha AM, Wilds CJ. Preparation of Covalently Linked Complexes Between DNA and O⁶-Alkylguanine-DNA Alkyltransferase Using Interstrand Cross-linked DNA. *Bioconjugate Chem.* 2013; 24:224–233.
32. Chen W, Schuster GB. Structural Stabilization of DNA-Templated Nanostructures: Cross-linking with 2,5-Bis(2-thienyl)-pyrrole Monomers. *Org Biomol Chem.* 2013; 11:35–40. [PubMed: 23086526]
33. Altmann S, Labhardt AM, Bur D, Lehmann C, Bannwarth W, Billeter M, Wüthrich K, Leupin W. NMR Studies of DNA Duplexes Singly Cross-linked by Different Synthetic Linkers. *Nucleic Acids Res.* 1995; 23:4827–4835. [PubMed: 8532525]
34. Glick G. Design, Synthesis, and Analysis of Conformationally Constrained Nucleic Acids. *Biopolymers.* 1998; 48:83–96. [PubMed: 9846126]
35. Ye M, Guillaume J, Liu Y, Sha R, Wang R, Seeman NC, Canary JW. Site Specific Inter-strand Cross-links of DNA Duplexes. *Chem Sci.* 2013; 4:1319–1329. [PubMed: 23894693]
36. Rajendran A, Endo M, Katsuda Y, Hidaka K, Sugiyama H. Photo-cross-linking-assisted Thermal Stability of DNA Origami Structures and its Application for Higher-temperature Self Assembly. *J Am Chem Soc.* 2011; 133:14488–14491. [PubMed: 21859143]
37. Varela JG, Gates KS. A Simple, High-Yield Synthesis of DNA Duplexes Containing a Covalent, Thermally-Reversible Interstrand Cross-link At a Defined Location. *Angew Chem Int Ed Eng.* 2015; 54:7666–7669.
38. Kasianowicz JJ, Brandin E, Branton D, Deamer DW. Characterization of Individual Polynucleotide Molecules Using a Membrane Channel. *Proc Nat Acad Sci USA.* 1996; 93:13770–13773. [PubMed: 8943010]
39. Song L, Hobaugh MR, Shustak C, Cheley S, Bayley H, Gouaux JE. Structure of Staphylococcal α -Hemolysin, a Heptameric Transmembrane Pore. *Science.* 1996; 274:1859–1865. [PubMed: 8943190]
40. Wanunu M. Nanopores: A Journey Towards DNA Sequencing. *Phys Life Rev.* 2012; 9:125–158. [PubMed: 22658507]

41. Wang Y, Tian K, Hunter LL, Ritzo B, Gu LQ. Probing Molecular Pathways for DNA Orientational Trapping, Unzipping and Translocation in Nanopores by Using a Tunable Overhang Sensor. *Nanoscale*. 2014; 6:11372–11379. [PubMed: 25144935]
42. Zhang X, Wang Y, Fricke BL, Gu LQ. Programming Nanopore Ion Flow for Encoded Multiplex microRNA Detection. *ACS Nano*. 2014; 8:3444–3450. [PubMed: 24654890]
43. Dutta S, Chowdhury G, Gates KS. Interstrand Crosslinks Generated by Abasic Sites in Duplex DNA. *J Am Chem Soc*. 2007; 129:1852–1853. [PubMed: 17253689]
44. Johnson KM, Price NE, Wang J, Fekry MI, Dutta S, Seiner DR, Wang Y, Gates KS. On the Formation and Properties of Interstrand DNA-DNA Cross-links Forged by Reaction of an Abasic Site With the Opposing Guanine Residue of 5'-CAp Sequences in Duplex DNA. *J Am Chem Soc*. 2013; 135:1015–1025. [PubMed: 23215239]
45. Catalano MJ, Liu S, Andersen N, Yang Z, Johnson KM, Price NA, Wang Y, Gates KS. Chemical Structure and Properties of the Interstrand Cross-link Formed by the Reaction of Guanine Residues with Abasic Sites in Duplex DNA. *J Am Chem Soc*. 2015; 137:3933–3945. [PubMed: 25710271]
46. Price NE, Catalano MJ, Liu S, Wang Y, Gates KS. Chemical and Structural Characterization of Interstrand Cross-links Formed Between Abasic Sites and Adenine Residues in Duplex DNA. *Nucleic Acids Res*. 2015; 43:3434–3441. [PubMed: 25779045]
47. Price NE, Johnson KM, Wang J, Fekry MI, Wang Y, Gates KS. Interstrand DNA DNA Cross-Link Formation Between Adenine Residues and Abasic Sites in Duplex DNA. *J Am Chem Soc*. 2014; 136:3483–3490. [PubMed: 24506784]
48. Maglia G, Henricus M, Wyss R, Li Q, Cheley S, Bayley H. DNA Strands from Denatured Duplexes are Translocated Through Engineered Protein Nanopores at Alkaline pH. *Nano Lett*. 2009; 9:3831–3836. [PubMed: 19645477]
49. Spanswick VJ, Hartley JM, Hartley JA. Measurement of DNA Interstrand Cross-linking in Individual Cells Using the Single Cell Electrophoresis. *Methods Mol Biol*. 2010; 613:267–282. [PubMed: 19997890]
50. Hartley JM, Spanswick VJ, Gander M, Giacomini G, Whelan J, Souhami RL, Hartley JA. Measurement of DNA Cross-linking in Patients on Ifosfamide Therapy Using the Single Cell Gel Electrophoresis (Comet) Assay. *Clin Cancer Res*. 1999; 5:507–512. [PubMed: 10100700]
51. Wu J, Clingen PH, Spanswick VJ, Mellinas-Gomez M, Meyer T, Puzanov I, Jodrell D, Hochhauser D, Hartley JA. γ -H2AX Foci Formation as a Pharmacodynamic Marker of DNA Damage Produced by DNA Cross-Linking Agents: Results from 2 Phase I Clinical Trials of SJG-136 (SG2000). *Clin Cancer Res*. 2012; 19:721–730. [PubMed: 23251007]
52. Ledermann JA, Gabra H, Jayson GC, Spanswick VJ, Rustin GJS, Jitlal M, James LE, Hartley JA, Claassen VP, Oltmann LF, et al. Inhibition of Carboplatin-Induced DNA Interstrand Cross-link Repair by Gemcitabine in Patients Receiving these Drugs for Platinum-Resistant Ovarian Cancer. *Clin Cancer Res*. 2010; 16:4899–4905. [PubMed: 20719935]
53. Fikrova P, Stetina R, Hrnčiarik M, Rehacek V, Jost P, Hronek M, Zadák Z, Claassen VP, Oltmann LF, Van't Riet J, et al. Detection of DNA Crosslinks in Peripheral Lymphocytes Isolated from Patients Treated with Platinum Derivatives Using Modified Comet Assay. *Neoplasma*. 2013; 60:413–418. [PubMed: 23581413]
54. McKenna DJ, McKeown SR, McKelvey-Martin VJ. Potential Use of the Comet Assay in the Clinical Management of Cancer. *Mutagenesis*. 2008; 23:183–190. [PubMed: 18256034]
55. Sambrook, J.; Fritsch, EF.; Maniatis, T. *Molecular Cloning: A Lab Manual*. Cold Spring Harbor Press; Cold Spring Harbor, NY: 1989.
56. Varshney U, van de Sande JH. Specificities and Kinetics of Uracil Excision from Uracil-Containing DNA Oligomers by *Escherichia coli* Uracil DNA Glycosylase. *Biochemistry*. 1991; 30:4055–4061. [PubMed: 2018771]
57. Lindahl T, Ljunquist S, Siegert W, Nyberg B, Sperens B. DNA N-Glycosidases: Properties of Uracil-DNA Glycosidase from *Escherichia coli*. *J Biol Chem*. 1977; 252:3286–3294. [PubMed: 324994]

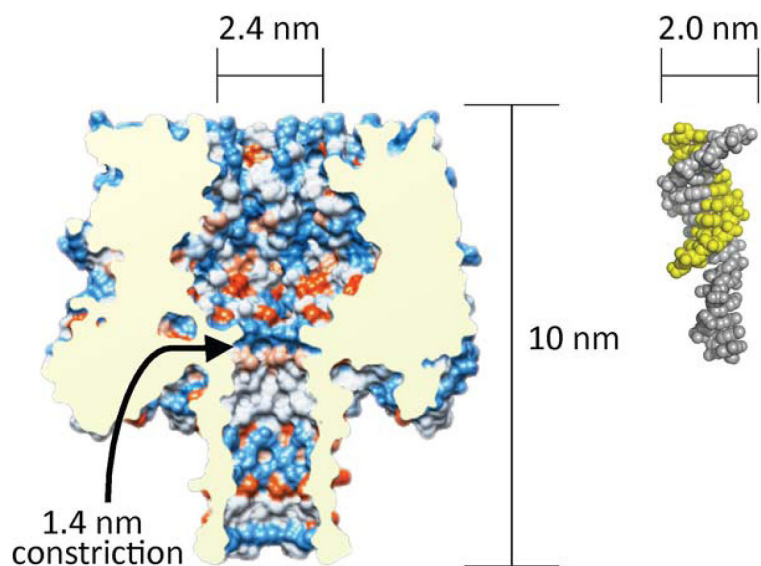


Figure 1. A cutaway view of the α -HL protein nanopore showing the critical dimensions alongside a 10 bp DNA duplex with a 6 nt overhang. The α -HL image was prepared from pdb 7AHL using the program Chimera and the DNA duplex image was prepared from pdb 3BSE using Pymol.

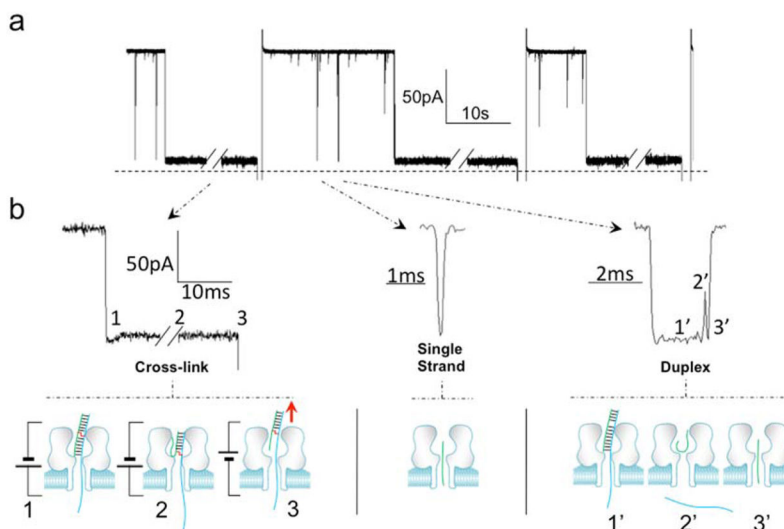


Figure 2.

Cross-linked duplex D7 causes a persistent current block in the α -HL nanopore. **a.** Analysis of an actual cross-linking reaction mixture containing cross-linked duplex, un-cross-linked duplex, and residual single-stranded DNA at 120 mV in Tris-HCl (10 mM, pH 7.4) containing KCl (1 M) at 22 ± 1 °C. Three types of blocking events are observed in the cross-linking reaction mixture: very short translocation events, dsDNA unzipping events, and persistent blocks by the cross-linked duplex. **b.** Expanded views of the current blocking events generated by cross-linked DNA, single strand DNA, and duplex DNA (from left to right). Both duplex and cross-linked DNA show three blocking levels. Beneath each current signature is a cartoon illustration showing the proposed molecular events responsible for each state. Left side: For the cross-linked DNA, state **1** corresponds to the poly-dC₃₀ tail threaded into the pore and the duplex in the vestibule, state **2** corresponds to the partially unzipped cross-link wedged at the constriction of the pore and, in state **3**, a reverse potential can be applied to “back” the DNA cross-link out of the pore to the *cis* side. Center: Single strand DNA will go through nanopore very quickly and will cause only one blocking level. Right side: when a dsDNA molecule is captured in the nanopore, state **1'** corresponds to the poly-dC₃₀ tail threaded into the pore and the duplex in the vestibule, state **2'** corresponds to unzipped duplex leaving the short strand of the duplex in the vestibule and, finally, state **3'** corresponds to the rapid translocation of the short strand through the pore.

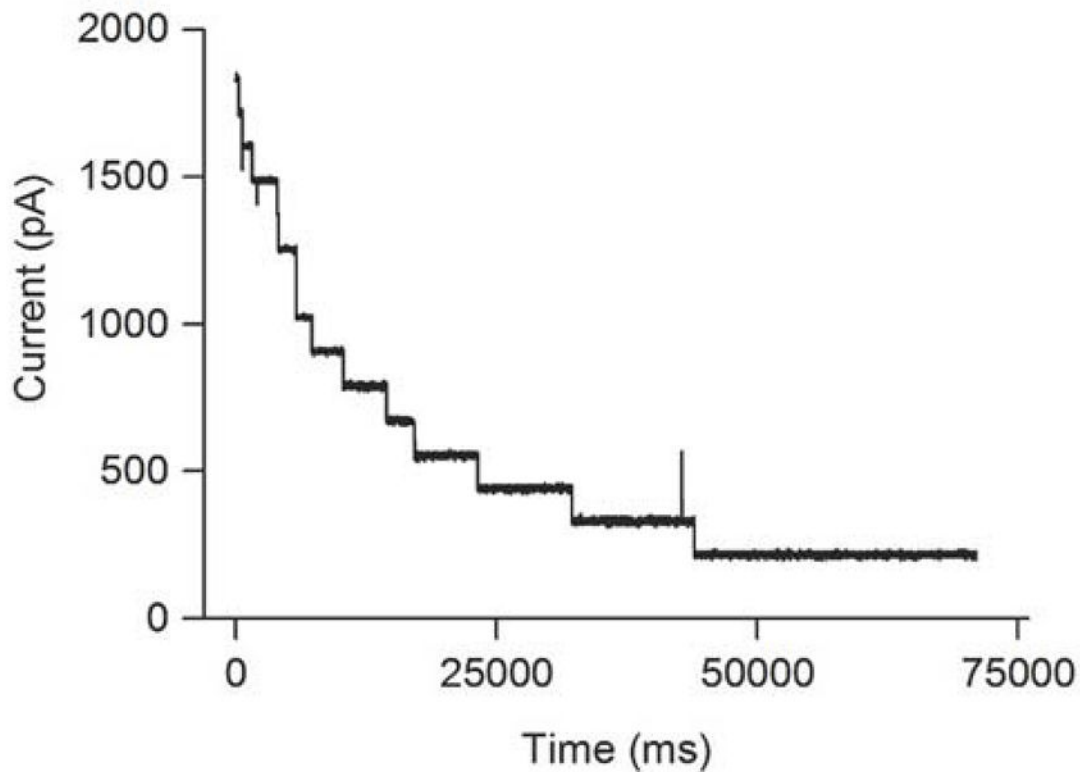
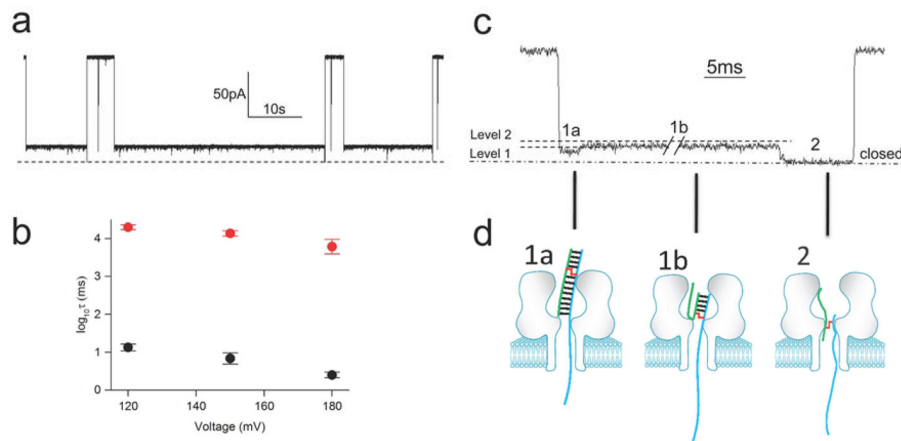


Figure 3. When multiple channels are present in the lipid bilayer, the cross-linked duplex D7 sequentially and irreversibly blocks the pores to cause an exponential decrease in current. This experiment was carried out on an actual cross-linking reaction containing cross-linked duplex, un-cross-linked duplex, and residual single-stranded DNA at 120 mV in Tris-HCl (10 mM, pH 7.4) containing KCl (1 M) at 22 ± 1 °C.

**Figure 4.**

Capture of the cross-linked duplex D3 in the α -HL nanopore generates a long-lasting current block, followed by translocation of the cross-linked DNA in Tris-HCl (10 mM, pH 7.4) containing KCl (1 M) at 22 ± 1 °C. **a.** Single channel recording of a cross-linking reaction mixture containing the D3 cross-link. **b.** Relationship between dwell time and applied voltage for passage of the un-cross-linked version of duplex D3 (black) and the cross-linked duplex D3 (red) through the α -HL nanopore. **c.** Expanded view of typical blocking events observed in the D3 cross-link mixture. The vertical scale of this panel is the same as in panel a. **d.** Beneath each current signature is a cartoon illustration showing the proposed molecular events responsible for each state.

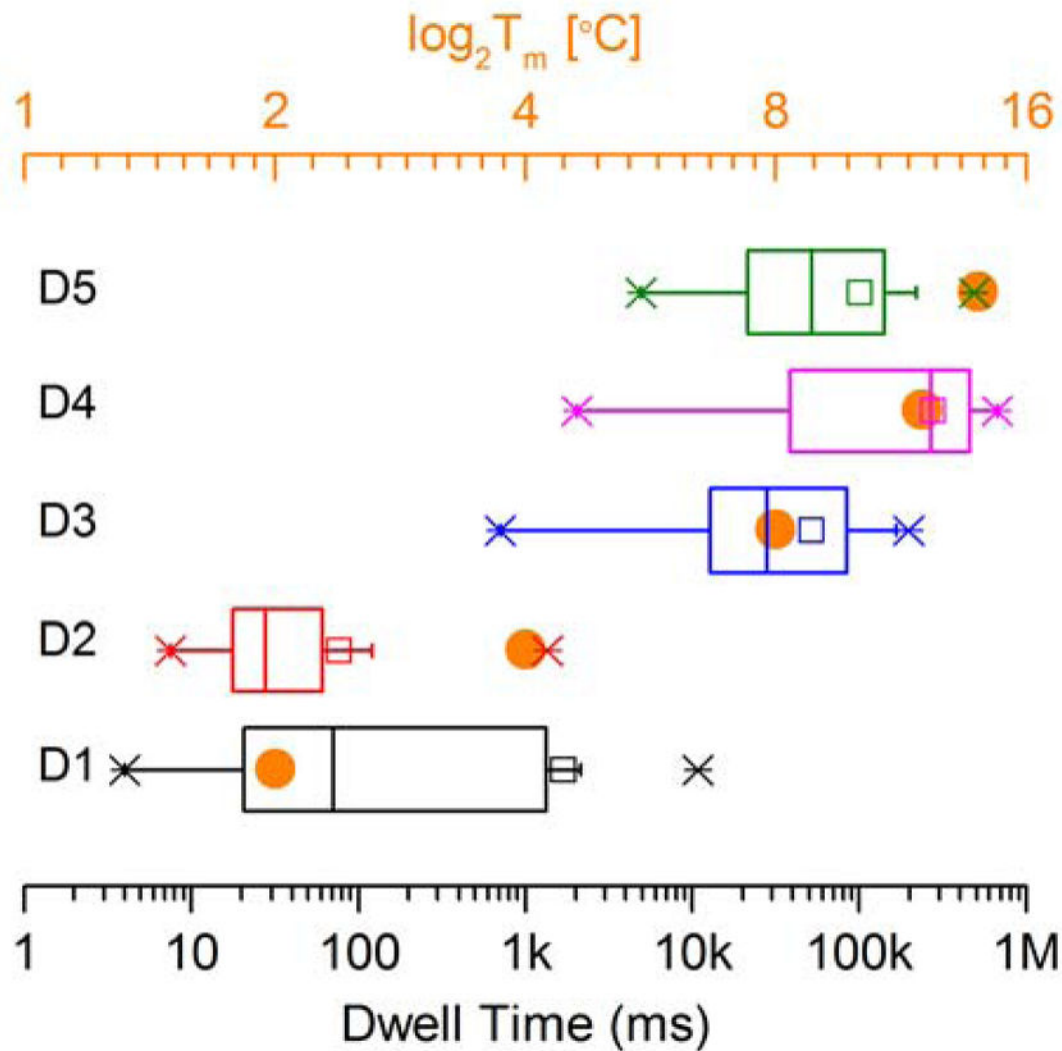


Figure 5.

Box chart showing that dwell times for duplexes D1-D5 correlate with the calculated melting temperature (T_m) of the residual duplex region left in the vestibule of the α -HL nanopore after partial unzipping of the cross-linked DNA. The orange dots are the calculated melting temperatures (T_m) shown in Table 1; the X's indicate the limits inside of which 99% of the data resides; the width of the box indicates the limits inside of which 50% of the data resides; the vertical line inside the box is the median value; the horizontal line indicates the size of the standard deviation; the hollow square marker is the mean value; the short horizontal line near the X-markers correspond to the minima and maxima values measured for the dwell times of each duplex.

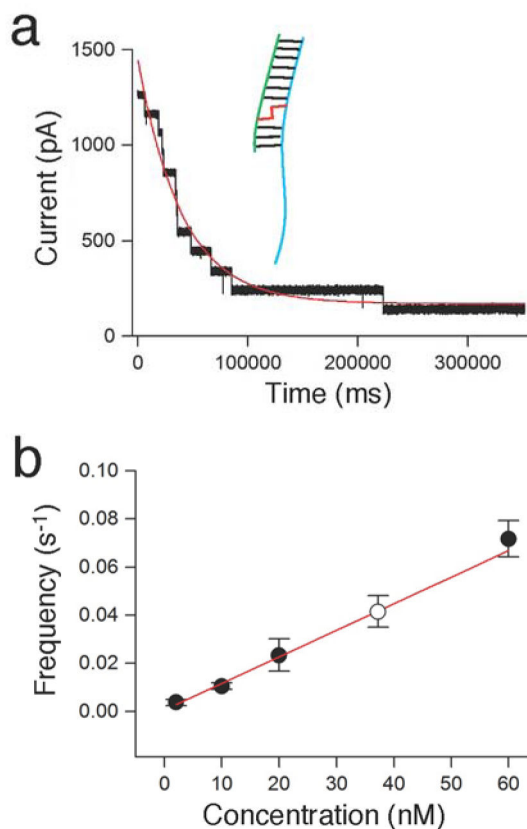
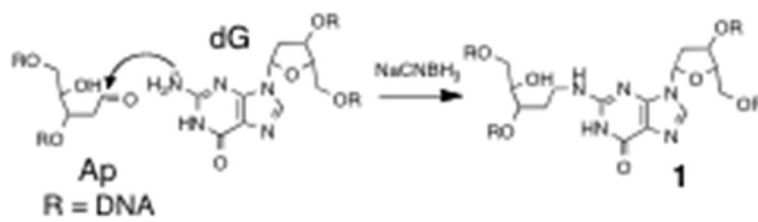


Figure 6.



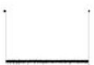





Quantitative analysis of cross-linked DNA. Panel **a**. A multi-channel nanopore experiment for counting the purified, cross-linked duplex D7 that cannot translocate through the nanopore at 120 mV in Tris-HCl (10 mM, pH 7.4) containing KCl (1 M) at 22 ± 1 °C. The nanopores are sequentially and irreversibly blocked by the cross-link. The frequency can be calculated from the exponential decrease in current flow. Panel **b**. Calibration curve showing the event frequency *versus* concentration for purified D7 cross-link. The solid circles are from multi-channel nanopore experiments and the value of empty circle is from a single channel experiment carried out at 40 nM concentration of cross-linked DNA.



Scheme 1.

Table 1

Cross-linked DNA sequences used in these studies. The red nucleotides indicate the site of cross-linking in the duplex. The melting temperatures correspond to the calculated T_m of the “residual duplex” (colored in blue) anticipated to remain in the vestibule of the α -HL nanopore following threading of the dC₃₀ tail and partial unzipping of the cross-linked substrate. The right-hand column shows representative current signatures of the blocks generated by each cross-link.

#	DNA Cross-Link Sequences ^a	Melting Temperature ^b	Typical Events
D1	5'-TTA AAT GAA CTA AGA CXA AAA 3'-C ₃₀ AAT TTA CTT GAT TCT GAT AAA	2 °C	 100ms
D2	5'-TTA AAT GAA CTA AGA CAC XTA 3'-C ₃₀ AAT TTA CTT GAT TCT GTG AAT	4 °C	 100ms
D3	5'-TTA AAT GAA CTA AGA CXA ATA 3'-C ₃₀ AAT TTA CTT GAT TCT GAT TAT	8 °C	 10s
D4	5'-TTA AAT GAA CTA ACX AAT ATA 3'-C ₃₀ AAT TTA CTT GAT TGA TTA TAT	12 °C	 200s
D5	5'-TTA AAT GAA CTA AGA CXA GCG 3'-C ₃₀ AAT TTA CTT GAT TCT GAT CGC	14 °C	 50s
D6	5'-TTA AAT GAA CXT AGA CAT ATA 3'-C ₃₀ AAT TTA CTT GAA TCT GTA TAT	22 °C	 10min
D7	5'-TTA AAT GAA CXA AGA CAT ATA 3'-C ₃₀ AAT TTA CTT GAT TCT GTA TAT	25 °C	 10min
D8	5'-TTA CXA GAA CTA AGA CAT ATA 3'-C ₃₀ AAT GAT CTT GAT TCT GTA TAT	50 °C	 10min

^aG-X corresponds to **1** in Scheme 1.

^bCalculated melting temperature of the residual duplex region (in blue) left in the vestibule of the nanopore after partial unzipping of the cross-linked substrate.